

# Quantum Monte Carlo calculations of neutron-alpha scattering

Kenneth M. Nollett,<sup>\*</sup> Steven C. Pieper,<sup>†</sup> and R. B. Wiringa<sup>‡</sup>  
*Physics Division, Argonne National Laboratory, Argonne, Illinois 60439*

J. Carlson<sup>§</sup> and G. M. Hale<sup>¶</sup>  
*Theoretical Division, Los Alamos National Laboratory, Los Alamos, NM 87545*  
(Dated: July 12, 2018)

We describe a new method to treat low-energy scattering problems in few-nucleon systems, and we apply it to the five-body case of neutron-alpha scattering. The method allows precise calculations of low-lying resonances and their widths. We find that a good three-nucleon interaction is crucial to obtain an accurate description of neutron-alpha scattering.

PACS numbers: 21.60.Ka, 25.10.+s, 21.45.+v, 27.10.+h

There has been significant progress recently in understanding the ground and low-lying excited states of light nuclei through microscopic calculations with realistic two- and three-nucleon interactions [1, 2, 3]. These studies have highlighted the importance of including a three-nucleon interaction to obtain correct overall binding of the p-shell nuclei [1], the ordering of states in  $^{10,11,12}\text{B}$  [3], and the stability of neutron-rich nuclei [4]. Modern calculations have been very successful in reproducing a large number of the experimentally-observed nuclear levels up to mass 12.

A wealth of additional experimental information is available in the form of low-energy scattering and reaction data. Very narrow low-energy resonances have been treated in the calculations discussed above as essentially bound states, but non-resonant scattering and broad resonances have not been adequately addressed. These cases require the development of methods to compute scattering states, which in turn will form the foundation for a quantitative, microscopic theory of low-energy nuclear reactions on light nuclei. Such a theory would be useful to astrophysics, because experimental determinations of crucial reaction rates are often difficult and sometimes impossible.

Here we review the method previously used for quantum Monte Carlo (QMC) calculations of low-energy reaction properties, present an improved method, and use it to study low-energy neutron-alpha scattering as a five-body problem. We evaluate the two low-lying  $p$ -wave resonances with  $J^\pi=3/2^-$  and  $1/2^-$ , respectively, as well as low-energy  $s$ -wave ( $1/2^+$ ) scattering.

In each case, we calculate the phase shift as a function of energy for the Argonne  $v_{18}$  (AV18) two-nucleon potential [5] alone, and with either the Urbana IX (UIX) model [6] or Illinois-2 (IL2) model [4] three-nucleon potential added. We find significant differences in the calculated phase shifts among these Hamiltonians. The AV18 and AV18+UIX models produce too little splitting of the  $3/2^-$  and  $1/2^-$  states, while AV18+IL2 reproduces their energies and widths very well. All three models provide good matches to the low-energy  $s$ -wave cross sections.

The results demonstrate that experimental phase shifts can be reproduced using realistic interactions with simple modifications to the computational method used for bound states. They also suggest that scattering calculations could provide sensitive constraints on models of the three-nucleon interaction.

In general it is very difficult to treat quantum scattering problems with more than a very few constituents. Often there are many initial or final states, and it is not yet possible to discretize the Schrödinger equation and solve directly for the scattering states. Correct treatment of the boundary conditions for more than two outgoing constituents is also complicated.

For low-energy scattering, though, there are often only a few two-cluster channels open. For one open channel of total angular momentum  $J$  and orbital angular momentum  $L$ , the wave function at large separation  $r$  of clusters with internal wave functions  $\Phi_{c1}$  and  $\Phi_{c2}$  will behave as

$$\Psi \propto \frac{1}{kr} \{ \Phi_{c1} \Phi_{c2} Y_L \}_J [ \cos \delta_{JL} F_L(kr) + \sin \delta_{JL} G_L(kr) ] , \quad (1)$$

where  $\delta_{JL}$  is the phase shift,  $k = \sqrt{2\mu E/\hbar^2}$ ,  $E$  is the scattering energy in the c.m. frame,  $\mu$  is the reduced mass,  $F_L$  and  $G_L$  are respectively regular and irregular real solutions of the Schrödinger equation with zero nuclear potential,  $Y_L$  are spherical harmonics, and  $\{\dots\}_J$  denotes angular momentum coupling.

Previous quantum Monte Carlo calculations of scattering states converted the scattering problem to an eigenvalue problem by imposing a boundary condition  $\Psi(r=R_0)=0$  at a surface radius  $R_0$  beyond the range of the nuclear interaction, and then solving for the energy within this nodal surface [7, 8]. Eq. (1) then gives  $\tan \delta_{JL} = -F_L(kR_0)/G_L(kR_0)$ . Finding  $E$  as a function of  $R_0$  is then equivalent to determining  $\delta_{JL}(E)$ .

The zero boundary condition requires different  $R_0$  for different scattering energies. Energies near threshold require very large  $R_0$ , which can cause numerical difficulties. For these reasons, it is preferable instead to impose a logarithmic derivative  $\gamma$  on the wave function along the

direction  $\hat{\mathbf{n}}$  normal to the  $r = R_0$  surface:

$$\hat{\mathbf{n}} \cdot \nabla_{\mathbf{r}} \Psi = \gamma \Psi, \quad \text{at } r = R_0. \quad (2)$$

Equation (1) then gives  $\delta_{JL}$  from  $E$ ,  $R_0$ , and  $\gamma$ .

We compute nuclear energies by using two QMC methods as successive approximations. The variational Monte Carlo (VMC) method uses a trial wave function  $\Psi_T(J^\pi; T)$  specified by variational parameters that are adjusted to minimize the energy expectation value; Monte Carlo techniques are used to evaluate the integrals over particle position. The method and the form of  $\Psi_T$  are described in detail in Refs. [1, 9]. VMC calculations of  $n$ - $\alpha$  scattering were first made in the 1980s [10], by using a  $\Psi_T$  that explicitly went to zero at  $R_0$ . In the present work, correlations inside  $\Psi_T$  are constrained so that it goes to the form Eq. (1) at large  $r$  and satisfies Eq. (2).

Green's function Monte Carlo (GFMC) takes the VMC trial state and evolves it in imaginary time  $\tau$ ,

$$\Psi(\tau) = \exp[-(H - E_0)\tau] \Psi_T, \quad (3)$$

so that  $\Psi(\tau \rightarrow \infty) \propto \Psi_0$ , the lowest state with the specified quantum numbers. The propagation time is divided into many small steps of length  $\Delta\tau$ , and Eq. (3) is computed by iterating the small-time-step Green's function,

$$G(\mathbf{R}', \mathbf{R}) = \langle \mathbf{R}' | \exp[-(H - E_0)\Delta\tau] | \mathbf{R} \rangle, \quad (4)$$

acting on samples of  $\Psi_T$ . Here  $\mathbf{R} = (\mathbf{r}_1, \mathbf{r}_2, \dots, \mathbf{r}_A)$  is the spatial configuration of the nucleons, and we suppress spin-isospin labels for simplicity. The nuclear GFMC method is described in Refs. [1, 9]. GFMC calculations with the nodal condition at  $R_0$  have been performed for  $n$ - $\alpha$  scattering previously [11] and also recently for some atomic and condensed-matter problems [12, 13].

In this work, we restrict the GFMC simulation to cluster separations less than  $R_0$  by rejecting proposed Monte Carlo steps that go outside the boundary. To enforce the boundary condition in Eq. (2), we regard the wave function in the restricted volume as the central region of a scattering wave function that fills all space, with some energy specified implicitly by the boundary condition. Then the contributions to  $\Psi(\tau)$  at the  $(n+1)$ th step in  $\tau$  come from inside and outside the  $r < R_0$  region:

$$\begin{aligned} \Psi_{n+1}(\mathbf{R}') &= \int_{|\mathbf{r}| < R_0} d\mathbf{R}_{c1} d\mathbf{R}_{c2} d\mathbf{r} G(\mathbf{R}', \mathbf{R}) \Psi_n(\mathbf{R}) \\ &+ \int_{|\mathbf{r}_e| > R_0} d\mathbf{R}_{c1} d\mathbf{R}_{c2} d\mathbf{r}_e G(\mathbf{R}', \mathbf{R}) \Psi_n(\mathbf{R}). \end{aligned} \quad (5)$$

Here  $\mathbf{R}$  is written in terms of both internal cluster coordinates  $\mathbf{R}_{c1}$  and  $\mathbf{R}_{c2}$ , and the cluster-cluster separations  $\mathbf{r}$  and  $\mathbf{r}_e$ , which respectively are contained inside, or extend outside, of the boundary  $R_0$ .

The contribution of the outer region can be mapped to an integral over the interior region by a change of

variables,  $\mathbf{r} = (R_0/r_e)^2 \mathbf{r}_e$  with  $r_e = |\mathbf{r}_e|$ , in the second term of Eq. (5). A wave function sample at the point  $\mathbf{R}'$  is then the sum of one contribution from the previous point  $\mathbf{R}$  and one from an ‘‘image point’’ at  $\mathbf{R}_e$ , located outside the  $r = R_0$  boundary:

$$\begin{aligned} \Psi_{n+1}(\mathbf{R}') &= \int_{|\mathbf{r}| < R_0} d\mathbf{R}_{c1} d\mathbf{R}_{c2} d\mathbf{r} G(\mathbf{R}', \mathbf{R}) \\ &\times \left[ \Psi_n(\mathbf{R}) + \frac{G(\mathbf{R}', \mathbf{R}_e)}{G(\mathbf{R}', \mathbf{R})} \left( \frac{r_e}{r} \right)^3 \Psi_n(\mathbf{R}_e) \right]. \end{aligned} \quad (6)$$

Because  $G(\mathbf{R}', \mathbf{R})$  has short range, we can use the boundary condition to obtain  $\Psi_n(\mathbf{R}_e)$  by linear extrapolation,

$$\Psi_n(\mathbf{R}_e) \approx [1 + \gamma(\mathbf{R}_e - \mathbf{R}) \cdot \hat{\mathbf{n}}] \Psi_n(\mathbf{R}), \quad (7)$$

or by fixing the energy and extrapolating with Eq. (1). The GFMC simulation considers each partition of the nucleons into clusters with separation  $\mathbf{r}$ . If the resulting  $|\mathbf{r} - \mathbf{r}_e| < 1$  fm, then the image contribution is used; otherwise the short range of  $G$  makes it insignificant.

This method has several advantages over the nodal boundary condition. The most important is that  $R_0$  can be set to a constant value, independent of the scattering energy. It is also possible to calculate correlated energy differences in the GFMC method for different values of the boundary condition if they are all computed for the same  $R_0$ . In such cases the path integrals differ only at the surface, and the energy differences are more accurate than the individual energies.

Neutron-alpha scattering provides a convenient test of several important properties of low-energy nuclear scattering. There is no bound state in the  $A=5$  system, but the  $3/2^-$  channel has a sharp low-energy resonance. The  $1/2^-$  state is broader and higher in energy, and the combination of these two states provides a simple measure of spin-orbit splitting. Since the alpha particle is so tightly bound, simple single-channel scattering continues up to fairly high energies.

The quantity most naturally given by a GFMC calculation is the total energy of a system, and a precision in the vicinity of 1% has been the goal of our past calculations. However, the quantity used to compute phase shifts is the energy relative to threshold, so a precision of 100 keV in this quantity is  $\sim 0.3\%$  of the total energy in the  ${}^5\text{He}$  problem. To attain this, we must pay close attention to the choice of  $R_0$ , construct a  $\Psi_T$  as close as possible to the desired GFMC solution, and use a less stringent GFMC path constraint.

First, the only *a priori* constraint on  $R_0$  is that it should be ‘‘beyond the range’’ of the nuclear interaction. We find that our GFMC result depends on  $R_0$  at the level of about 100 keV (out of a total of  $\sim -28$  MeV) in going from  $R_0 = 7$  fm to 9 fm. We find no further change going from 9 fm to 10 fm; the highest attainable energy (corresponding to the state with a node at the surface) decreases as  $R_0$  increases, so we choose  $R_0 = 9$

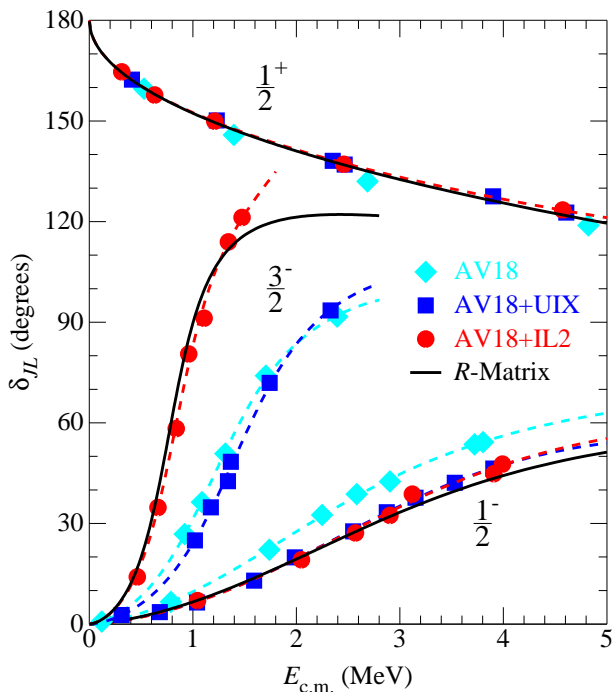


FIG. 1: (Color online) Phase shifts for  $n$ - $\alpha$  scattering. Filled symbols (with statistical errors smaller than the symbols) are GFMC results; dashed curves are fits described in the text; and solid curves are from an  $R$ -matrix fit to data [14].

fm. Future calculations extending to energies beyond this maximum-energy state should be analogous to previous calculations of multiple bound states with the same quantum numbers [15].

Second, the GFMC energy also depends somewhat on the input  $\Psi_T$ . We find it important to adjust pair correlations between particles in different clusters (between the  $n$  and constituents of the  $\alpha$  in this case) so that Eq. (1) is enforced at large cluster separation [16]. We also adjust a parameter in  $\Psi_T$  that corresponds to the scattering energy until it matches the final GFMC energy; this typically takes one or two iterations of the VMC and GFMC calculations to obtain a self-consistent result.

Finally, in all of our  $A > 4$  GFMC calculations, we use a path constraint [1] on the GFMC walk to mitigate the Fermion sign problem; we compute energy samples only after releasing the constraint for some number of steps to avoid biasing the results. We find that stable results in our scattering calculations require the use of 80 unconstrained steps rather than the usual 20 to 40.

In Fig. 1 we present phase shifts for all channels, computed with three different interaction models. In each case the AV18 potential is used as the two-nucleon interaction; in the second (third) case the UIX (IL2) three-nucleon potential is added. We also show partial-wave total cross sections for the AV18+IL2 case in Fig. 2. We compare these results with those from a multi-channel  $R$ -

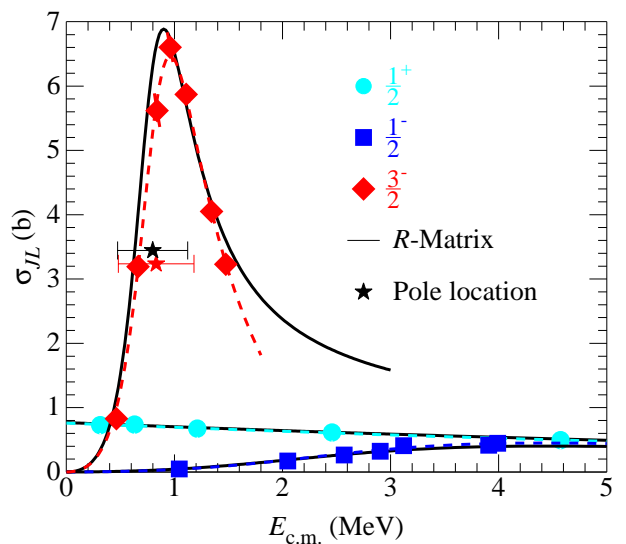


FIG. 2: (Color online) Calculated and  $R$ -matrix partial-wave cross sections. The calculations, shown with their Monte Carlo error bars, are for the AV18+IL2 Hamiltonian. Stars show the pole energies in  $3/2^-$  scattering for the  $R$ -matrix fit and for AV18+IL2, with the bars indicating the imaginary part.

matrix analysis of the  ${}^5\text{He}$  system [14] that characterizes the measured scattering data very well ( $\chi^2/\text{d.o.f.}$  is 1.6). Some of the resonance parameters from that analysis are given in Refs. [17] and [18]. Because there are more than 2600 data points in the analysis, the uncertainties in the  $R$ -matrix phase shifts are likely to be much smaller than the errors in the GFMC calculations.

We have made rational polynomial fits to  $\tan \delta_{JL}/k^{2L+1}$ , converted these to rational polynomials for the  $S$ -matrix, and used these to find the poles of  $S$ . These fits are shown as dashed curves in the figures. For each of the two  $p$ -wave states, we find just one pole that is stable as the degrees of the polynomials are changed; we identify these as the resonance poles. For  $3/2^-$  the poles are at  $1.19 - 0.77i$ ,  $1.39 - 0.75i$ , and  $0.83 - 0.35i$  for AV18 alone, AV18+UIX, and AV18+IL2, respectively, compared with  $0.798 - 0.324i$  MeV from analysis of the data [18]. The corresponding  $1/2^-$  values are  $1.7 - 2.2i$ ,  $2.4 - 2.5i$ , and  $2.3 - 2.6i$  MeV, compared with  $2.07 - 2.79i$  MeV. The  $1/2^+$  fits yield no stable pole, in agreement with the lack of a resonance in this channel and with the  $R$ -matrix analysis. We have quoted all pole locations, and the scattering length below, so that there is an error of not more than 3 in the last decimal place.

It is well known that realistic two-nucleon interactions alone provide insufficient spin-orbit splitting in light nuclei [19, 20]. The figures and pole positions above confirm this: although there is some spin-orbit splitting with AV18, it is less than half of what is needed to explain the data. The UIX three-nucleon potential includes a

two-pion-exchange term and a phenomenological short-range repulsion, fitted simultaneously to the triton binding energy and the saturation density of nuclear matter. Adding UIX to AV18 increases the spin-orbit splitting, but not enough to match the data.

In addition to the terms in the UIX model, the IL2 potential includes a three-pion-ring exchange term and an additional two-pion-range term. The strengths of all four terms were adjusted to fit seventeen energy levels in nuclei up to  $A=8$  [4]. Adding IL2 to AV18 induces even greater spin-orbit splitting in the fitted nuclei; the figures and pole positions show that the experimental  ${}^5\text{He}$  splitting is almost exactly reproduced by AV18+IL2. For comparison, excitation energies for this interaction have an RMS deviation of 600 keV from experiment for the states to which it was fitted. The widths of the resonances are also well reproduced by AV18+IL2.

All three potentials produced essentially identical results for the  $1/2^+$  case, in good agreement with the laboratory data. The  $s$ -wave scattering is dominated by a node in the  $n$ - $\alpha$  correlation at a position that roughly fixes the zero-energy scattering length, and the wave functions for all potentials contain similar structure. All three are consistent with a scattering length of 2.4 fm, compared with an experimental scattering length of 2.46 fm [18].

In summary, we have introduced a new QMC technique to calculate low-energy scattering and applied it to neutron-alpha scattering. Models of the three-nucleon interaction that have been successful in describing bound levels of light nuclei also provide good descriptions of these scattering states. In the case of the most successful potential, AV18+IL2, the description is particularly good. The sensitivity of the results in Fig. 1 to the Hamiltonian suggests that scattering calculations can provide important additional constraints on the three-nucleon interaction. We note that the energies obtained here for the  $3/2^-$  pole are close to those obtained by treating it as a bound state [4], while the pseudo-bound-state calculations of the broad  $1/2^-$  state proved less reliable.

Many extensions and applications of the computational method presented here are possible. Because these calculations are done in coordinate space, including Coulomb interactions between the clusters will pose no problems; the  $F_L$  and  $G_L$  of Eq. (1) are then simply Coulomb, rather than Bessel, functions. Extensions to nucleus-nucleus (rather than nucleon-nucleus) scattering should also be feasible. Besides pure scattering problems and the use of scattering wave functions to compute electroweak cross sections [21] and hadronic parity violation, the scattering method should be applicable to cases with more than one open two-cluster channel. For  $N_{\text{ch}}$  such channels, a set of  $N_{\text{ch}}$  linearly independent solutions of the Schrödinger equation at the same energy determines the  $S$ -matrix. The solutions could be obtained either by varying the boundary conditions at the surface, or by

calculating the derivative of the energy with respect to changes in the logarithmic derivatives.

We gratefully acknowledge valuable discussions with V. R. Pandharipande. The many-body calculations were performed on the parallel computers of the Laboratory Computing Resource Center, Argonne National Laboratory and the National Energy Research Scientific Computing Center. The work of KMN, SCP, and RBW is supported by the U. S. Department of Energy, Office of Nuclear Physics, under contract No. DE-AC02-06CH11357. The work of JC and GMH is supported by the U. S. Department of Energy under contract No. DE-AC52-06NA25396.

---

\* Electronic address: nollett@anl.gov

† Electronic address: spieper@anl.gov

‡ Electronic address: wiringa@anl.gov

§ Electronic address: carlson@lanl.gov

¶ Electronic address: ghale@lanl.gov

- [1] R. B. Wiringa, S. C. Pieper, J. Carlson, and V. R. Pandharipande, Phys. Rev. C **62**, 014001 (2000).
- [2] S. C. Pieper, K. Varga, and R. B. Wiringa, Phys. Rev. C **66**, 044310 (2002).
- [3] P. Navrátil and W. E. Ormand, Phys. Rev. C **68**, 034305 (2003).
- [4] S. C. Pieper, V. R. Pandharipande, R. B. Wiringa, and J. Carlson, Phys. Rev. C **64**, 014001 (2001).
- [5] R. B. Wiringa, V. G. J. Stoks, and R. Schiavilla, Phys. Rev. C **51**, 38 (1995).
- [6] B. S. Pudliner, V. R. Pandharipande, J. Carlson, and R. B. Wiringa, Phys. Rev. Lett. **74**, 4396 (1995).
- [7] J. Carlson, V. R. Pandharipande, and R. B. Wiringa, Nucl. Phys. **A424**, 47 (1984).
- [8] Y. Alhassid and S. E. Koonin, Ann. Phys. (NY) **155**, 108 (1984).
- [9] B. S. Pudliner, V. R. Pandharipande, J. Carlson, S. C. Pieper, and R. B. Wiringa, Phys. Rev. C **56**, 1720 (1997).
- [10] J. Carlson, K. E. Schmidt, and M. H. Kalos, Phys. Rev. C **36**, 27 (1987).
- [11] J. Carlson, Nucl. Phys. **A522**, 185c (1991).
- [12] J. Shumway and D. M. Ceperley, Phys. Rev. B **63**, 165209 (2001).
- [13] S. Chiesa, M. Mella, and G. Morosi, Phys. Rev. A **66**, 042502 (2002); **69**, 022701 (2004).
- [14] G. M. Hale, D. C. Dodder, and K. Witte, unpublished (1995).
- [15] S. C. Pieper, R. B. Wiringa, and J. Carlson, Phys. Rev. C **70**, 054325 (2004).
- [16] K. M. Nollett, R. B. Wiringa, and R. Schiavilla, Phys. Rev. C **63**, 024003 (2001).
- [17] A. Csóto and G. M. Hale, Phys. Rev. C **55**, 536 (1997).
- [18] D. R. Tilley *et al.*, Nuc. Phys. **A708**, 3 (2002).
- [19] S. C. Pieper and V. R. Pandharipande, Phys. Rev. Lett. **70**, 2541 (1993).
- [20] J. Fujita and H. Miyazawa, Prog. Theor. Phys. **17**, 360 (1957); **17**, 366 (1957).
- [21] L. E. Marcucci, K. M. Nollett, R. Schiavilla, and R. B. Wiringa, Nucl. Phys. **777**, 111 (2006).